

UC Berkeley

UC Berkeley Previously Published Works

Title

High-titer production of lathyrane diterpenoids from sugar by engineered *Saccharomyces cerevisiae*

Permalink

<https://escholarship.org/uc/item/6bw952k1>

Authors

Wong, Jeff
de Rond, Tristan
d'Espaux, Leo
et al.

Publication Date

2018

DOI

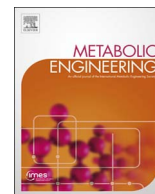
10.1016/j.ymben.2017.12.007

Peer reviewed



Contents lists available at ScienceDirect

Metabolic Engineering

journal homepage: www.elsevier.com/locate/meteng

High-titer production of lathyrane diterpenoids from sugar by engineered *Saccharomyces cerevisiae*

Jeff Wong^{a,b,c}, Tristan de Rond^{b,c,d}, Leo d'Espaux^{b,c}, Cas van der Horst^{b,c}, Ishaan Dev^{b,c,e},
Leo Rios-Solis^{b,c}, James Kirby^{b,c}, Henrik Scheller^{a,b}, Jay Keasling^{b,c,e,*}

^a Department of Plant and Microbial Biology, University of California, Berkeley, CA 94720, United States

^b DOE Joint BioEnergy Institute, Emeryville, CA 94608, United States

^c Biological Systems and Engineering Division, Lawrence Berkeley National Laboratory, Berkeley, CA 94720, United States

^d Department of Chemistry, University of California, Berkeley, CA 94720, United States

^e Department of Chemical Engineering and Bioengineering, University of California at Berkeley and Physical Biosciences Division, Lawrence Berkeley National Laboratory, and Joint BioEnergy Institute, Emeryville, CA, United States

A B S T R A C T

Euphorbiaceae are an important source of medically important diterpenoids, such as the anticancer drug ingenol-3-angelate and the antiretroviral drug prostratin. However, extraction from the genetically intractable natural producers is often limited by the small quantities produced, while the organic synthesis of terpene-derived drugs is challenging and similarly low-yielding. While transplanting the biosynthetic pathway into a heterologous host has proven successful for some drugs, it has been largely unsuccessful for diterpenoids due to their elaborate biosynthetic pathways and lack of genetic resources and tools for gene discovery. We engineered casbene precursor production in *S. cerevisiae*, verified the ability of six *Euphorbia lathyris* and *Jatropha curcas* cytochrome P450s to oxidize casbene, and optimized the expression of these P450s and an alcohol dehydrogenase to generate jolkinol C, achieving ~800 mg/L of jolkinol C and over 1 g/L total oxidized casbanes in milliliter plates, the highest titer of oxidized diterpenes in yeast reported to date. This strain enables the semisynthesis of biologically active jolkinol C derivatives and will be an important tool in the elucidation of the biosynthetic pathways for ingenanes, tiglanes, and lathyrans. These findings demonstrate the ability of *S. cerevisiae* to produce oxidized drug precursors in quantities that are sufficient for drug development and pathway discovery.

1. Introduction

A range of medicinal diterpenoid compounds (e.g., casbanes, lathyrans, jatrophanes, tiglanes, and ingenanes) produced solely in *Euphorbiaceae* and *Thymelaceae* plants have gained interest due to their unique anti-cancer, anti-HIV, vascular-relaxing, neuro-protective, anti-inflammatory, and immunomodulatory activities (Vasas and Hohmann, 2014; Srivalli and Lakshmi, 2012; Jiao et al., 2009; Halaweish et al., 2002; Wang et al., 2015). These compounds include ingenol-3-angelate, recently approved by the US FDA for the treatment of the premalignant skin condition actinic keratosis (Siller et al., 2009) (Fig. 1b); prostratin, in phase I clinical trials as an adjuvant therapy to clear latent viral reservoirs; and resiniferatoxin, studied for its powerful analgesic effects (Johnson et al., 2008; Payne et al., 2005). Indeed, the demand for medicinal diterpenoids is exemplified by the rise of paclitaxel and other *Taxus*-derived drugs, which is estimated to be a \$2.3 billion industry worldwide (Selling Forest Environmental Services, 2012).

The medicinal properties and unusual structures of lathyrane diterpenoids, a group of tricyclic diterpenes derived from the hydrocarbon casbene, as well as tiglane and ingenane diterpenes have led to many attempts at chemical synthesis and direct purification from plants (Vasas and Hohmann, 2014; Shimokawa et al., 2007; Wender and McDonald, 1990; Tanino et al., 2003). Prostratin is produced via a semisynthetic route, and ingenol-3-angelate by mass extraction from *Euphorbia peplus* plants. However, chemical synthesis is complicated by the multiple chiral centers in these diterpenoid compounds, while extraction from plant tissues is inefficient and costly, with yields typically in the range of 0.1–10% from starting material (Tanino et al., 2003; Wender et al., 2008). The development of a microbial production host for lathyrane diterpenoids could significantly reduce the production cost and increase the availability of these compounds. Such a host could also produce other medically important diterpenoids that are not produced naturally or at levels insufficient to detect.

Yeast is a particularly attractive host for microbial engineering

* Corresponding author at: DOE Joint BioEnergy Institute, Emeryville, CA 94608, United States.
E-mail address: keasling@berkeley.edu (J. Keasling).

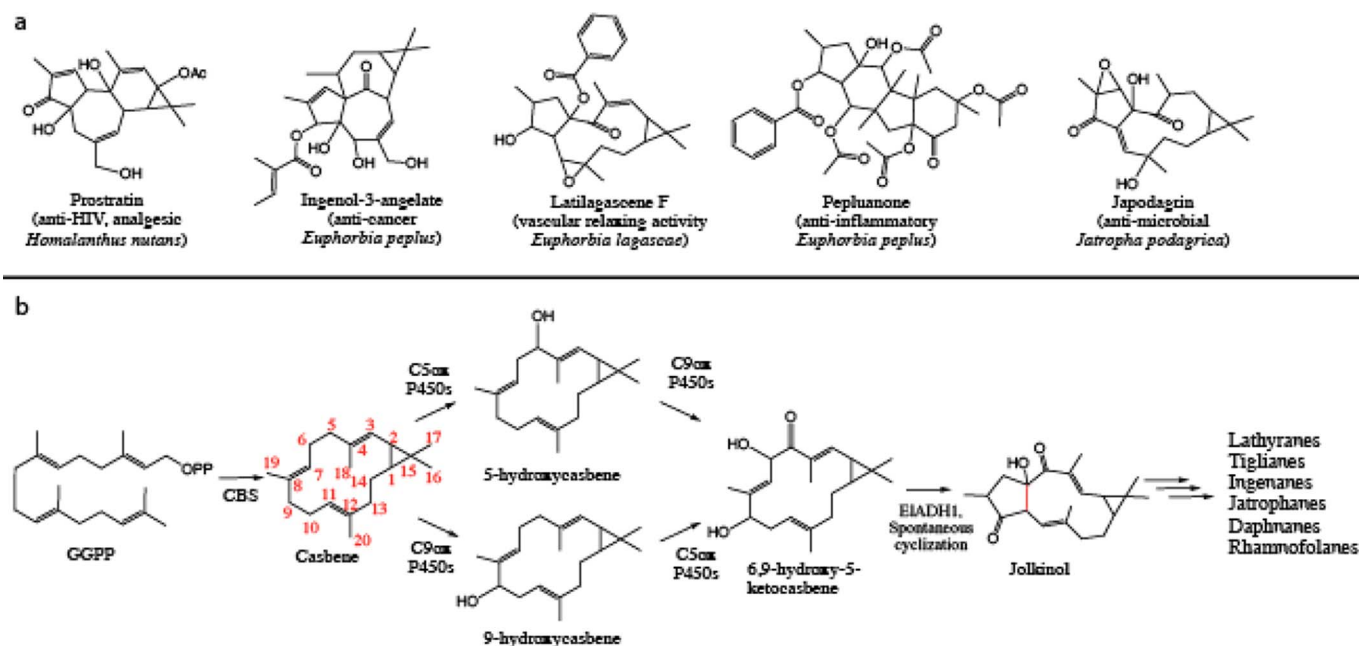


Fig. 1. *Euphorbiaceae* diterpenoid biosynthetic pathways originate from casbene. (a) Structures of bioactive *Euphorbiaceae* diterpenes. (b) Proposed pathway for the production of medicinal *Euphorbiaceae* diterpenoids begins with geranylgeranyl diphosphate (GGPP) from the DXPP pathway in plants, which is cyclized by casbene synthase (CBS) and subsequently oxidized by numerous P450s. Enzymes required to form jolkinol C in both *J. curcas* and *E. lathyris* have been functionally characterized. C9OX CYP (EICYP71D445p/JcCYP71D495p) homologs oxidize the C-9 position of casbene, while C5OX CYP (EICYP726A27p/JcCYP726A35p/JcCYP726A20p) homologs oxidize the C-5 position of casbene. Consequently, both enzymes have been shown to catalyze the hydroxylation of C-6 position of casbene. The formation of a carbonyl at position 5 n has been postulated to result in the tautomerization and spontaneous ring closure forming jolkinol C. Hamberger and colleagues have shown the necessity of the alcohol dehydrogenase ElAdh1p to form jolkinol C *in vitro* using *E. lathyris* enzymes (Luo et al., 2016). Additional steps towards production of decorated diterpenes are diverse and unknown.

because of its robustness in industrial fermentation and genetic tractability. The development of yeast strains producing > 10 g/L of the anti-malarial artemisinin acid has demonstrated the potential of using yeast as a heterologous host for oxidized natural product production (Paddon et al., 2013; Westfall et al., 2012). Development of monoterpenoid (C5) and diterpenoid (C20) production in yeast has lagged behind sesquiterpenoid (C15) production, with fewer studies and lower titers (< 20 mg/L and < 1 g/L, respectively) (Triikka et al., 2015; Ignea et al., 2014, 2011; Jongedijk et al., 2015; Amiri et al., 2016; Andersen-Ranberg et al., 2016).

The biosynthesis of lathyrane isoprenoids begins with the common five-carbon isoprenoid precursors IPP and DMAPP, which are sequentially condensed to form the universal 20-carbon isoprenoid intermediate geranylgeranyl-pyrophosphate (GGPP). A diterpene synthase found in several *Euphorbiaceae*, casbene synthase (CBS), cyclizes GGPP to form casbene (Fig. 1a) (Kirby et al., 2010). From casbene, the biosynthetic route to lathyrane isoprenoids is poorly understood, but is thought to proceed through intermediates such as jolkinol C via cytochrome P450-catalyzed oxidations and possibly a short-chain alcohol dehydrogenase (ADH). Different groups have debated the involvement of the ADH in the formation of jolkinol C; Luo and colleagues found that, in addition to the CYPs required to oxidize casbene, an *Euphorbia lathyris* ADH (ElAdh1) was necessary for jolkinol C formation in *N. benthamiana* and *in vitro* (Luo et al., 2016). In contrast, King and colleagues never mentioned the use of an ADH for the production of jolkinol C, but saw production of jolkinol C from coexpression of casbene synthase and two *Jatropha curcas* CYPs (King et al., 2016).

Reconstituting complex oxidized terpenoid biosynthetic pathways, such as those of lathyranes, in heterologous hosts has posed numerous problems requiring optimizing the expression of a cytochrome P450 reductase (CPR) and the CYP, as well as balancing the redox environment within the cell (Paddon et al., 2013; Renault et al., 2014). Indeed, only about 40% of all plant-derived CYPs tested in yeast express poorly if at all (Renault et al., 2014). It is important to note that yeast has proved to be a better host for CYP expression than prokaryotic hosts

such as *Escherichia coli* due to the presence of the endoplasmic reticulum in the former organism. A previous study found that despite the coexpression of the pathway enzymes required to produce jolkinol C in *Nicotiana benthamiana* and *in vitro*, coexpression of these enzymes in yeast did not result in jolkinol C formation (Luo et al., 2016). This research illustrates the need to engineer casbene and lathyrane pathways in yeast to aid functional testing of additional pathway enzymes.

The present work describes the establishment of yeast strains producing lathyrane diterpenoids as a platform for producing varied medicinal compounds. We have constructed a strain that synthesizes the lathyrane backbone casbene at high titer. We verified the ability of *E. lathyris* and *J. curcas* P450s to oxidize casbene, and resolved some discrepancies between the two pathways previously proposed (Luo et al., 2016; King et al., 2016). Finally, we optimized the expression of these P450s and an ADH to generate jolkinol C at high titers producing a strain with all pathway genes stably integrated as a chassis for additional gene discovery.

2. Materials and methods

2.1. Strain construction

The parent *Saccharomyces cerevisiae* strain used for all engineering was GTy116 {MATa, leu2-3, 112::HIS3MX6-GAL1p-ERG19/GAL10p-ERG8;ura3-52::URA3-GAL1p-MvaSA110G/GAL10p-MvaE (codon optimized); his3Δ1::hphMX4-GAL1p-ERG12/GAL10p-ID11; trp1-289::TRP1-GAL1p-CrtE(X.den)/GAL10p-ERG20;YPRCdelta15::NatMX-GAL1p-CrtE(opt)/GAL10p-CrtE} previously used by our lab (Reider Apel et al., 2017). The integration cassettes for all subsequent strains (Table 1, Supplementary Table 1) were created using the software tools CASdesigner (casdesigner.jbei.org) and DIVA(diva.jbei.org) and integrated using the previously reported, cloning-free methodology via Cas9-aided homologous recombination (Reider Apel et al., 2017). Integration cassettes containing 1-kb flanking homology regions targeting a chosen genomic locus were constructed by PCR amplifying donor

Table 1
Yeast strains and gene nomenclature.

Strain	Parent (+ additional genetic changes)	Compound	References
GTY116	<i>MATa leu2-3112::His3MX6_{P_{GAL1}}-ERG19/P_{GAL10}-ERG8 ura3-52::URA3_{P_{GAL1}}-mvaS(A110G)/P_{GAL10}-mvaE(CO) his3Δ1::hphMX4_{P_{GAL1}}-ERG12/P_{GAL10}-ID11 trp1-289::TRP1_{P_{GAL1}}-crtE(X.den)/P_{GAL10}-ERG20 yprcδ15::natMX_{P_{GAL1}}-crtE(opt)/P_{GAL10}-crtE</i>	GGPP	ref. Reider Apel et al. (2017)
JWY501	GTY116 (<i>ura3-52</i> prototrophy removed for use of Cas9 system)	GGPP	This work
JWY509	JWY501 (<i>ARS1622b::P_{GAL1}-CBS ARS1014a::P_{GAL1}-nMBP-CBS, P_{GAL10}-nGFP-CBS ARS308a::P_{GAL1}-nMBP-CBS-erg20F96c</i>)	Casbene	This work
JWY510	JWY509 (<i>ARS911b::P_{GAL10}-JcCPR1, P_{GAL1}-JcC9OX1</i>)	C-9 oxidized casbanes	This work
JWY511	JWY509 (<i>ARS911b::P_{GAL10}-JcCPR1, P_{GAL1}-JcC9OX2</i>)	C-9 oxidized casbanes	This work
JWY512	JWY509 (<i>ARS911b::P_{GAL10}-JcCPR1, P_{GAL1}-ElC9OX1</i>)	C-9 oxidized casbanes	This work
JWY513	JWY509 (<i>ARS911b::P_{GAL10}-JcCPR1, P_{GAL1}-ElC5OX1</i>)	C-5 oxidized casbanes	This work
JWY514	JWY509 (<i>ARS911b::P_{GAL10}-JcCPR1, P_{GAL1}-JcC5OX1</i>)	C-5 oxidized casbanes	This work
JWY515	JWY509 (<i>ARS911b::P_{GAL10}-JcCPR1, P_{GAL1}-JcC5OX2</i>)	C-5 oxidized casbanes	This work
JWY516	JWY512 (<i>ARS1021b::P_{GAL1}-JcC5OX2</i>)	Jolkinol	This work
JWY517	JWY512 (<i>ARS1021b::P_{GAL1}-JcC5OX1</i>)	Mix of C-5/C-9 oxidized casbanes	This work
JWY518	JWY512 (<i>ARS1021b::P_{GAL1}-ElC5OX1</i>)	Mix of C-5/C-9 oxidized casbanes	This work
JWY519	JWY511 (<i>ARS1021b::P_{GAL1}-JcC5OX2</i>)	Jolkinol	This work
JWY520	JWY516 (<i>HIS3b::P_{GAL1}-JcADH1</i>)	Jolkinol	This work
JWY521	JWY519 (<i>HIS3b::P_{GAL1}-JcADH1</i>)	Jolkinol	This work
Abbreviation	Published name		References
<i>JcCBS1</i>	<i>JcCSH</i>		ref. Nakano et al. (2012)
<i>JcC9OX1</i>	<i>JcCYP71D496</i>		ref. King et al. (2016)
<i>JcC9OX2</i>	<i>JcCYP71D495</i>		ref. King et al. (2016)
<i>ElC9OX1</i>	<i>ElCYP71D445</i>		ref. Luo et al. (2016)
<i>ElC5OX1</i>	<i>ElCYP726A20</i>		ref. Luo et al. (2016)
<i>JcC5OX1</i>	<i>JcCYP35a20</i>		ref. King et al. (2016)
<i>JcC5OX2</i>	<i>JcCYP726A20</i>		ref. King et al. (2016)

DNA fragments using primers generated by CASdesigner, then co-transformed with a Cas9-gRNA plasmid (pCut) targeting the chosen genomic locus. CASdesigner primers provide 30–60 nt of inter-fragment homology allowing 1–5 separate fragments to assemble via homologous recombination *in vivo*. pCuts targeting empty genomic loci (e.g., 208a, 1622b) were available pre-cloned, and pCuts targeting new sites (e.g., for deletions) were assembled *in vivo* from a linear backbone and a linear PCR fragment containing the new gRNA sequence, as described previously (Reider Apel et al., 2017). The new gRNA sequence for the URA3 locus (Suppl. Table 1) was chosen using DNA2.0 (www.dna20.com/eCommerce/cas9/input). To generate donor DNA fragments, native sequences—e.g., chromosomal homology regions, promoters—were amplified from CEN.PK2-1C genomic DNA, while heterologous sequences—e.g., P450 coding sequences (Supplementary Fig. 10)—were amplified from synthetic gene blocks codon-optimized (for expression in *S. cerevisiae*) and synthesized by Integrated DNA Technologies (www.idtdna.com).

All PCRs used Phusion Hot Start II DNA polymerase (www.thermofisher.com, cat. F549L). The following touchdown PCR cycling conditions were used for all PCRs: 1 cycle of 98 °C for 15 s; 25 cycles of 98 °C for 10 s, 65 °C for 30 s (dropping 1 degree each cycle after the first cycle), 72 °C for 30 s, and then 25 cycles of 98 °C for 10 s, 50 °C for 30 s, 72 °C for 30 s. Transformations were performed via heat-shock using ~200 ng pCut, ~1 μg donor DNA per sample, and 20 min heat shock at 42 °C, then plated all cells on selective agarose plates (Gietz and Woods, 2002). For assembling a pCut targeting a new site by homologous recombination, we used 200 ng linear pCut backbone and 500 ng of a 1-kb fragment containing the gRNA sequence, as described (Reider Apel et al., 2017). For multi-site integrations, we used 200 ng total linear pCut backbone, and the same amounts of gRNA fragment and donor DNA for each site as we would have for a single integration. Colonies were screened by PCR directed at the target locus, and for integrations, one representative colony sequenced. Three to four biological replicates were analyzed for each strain.

2.2. Development of chimeric JcCYP726A35

To produce a JcCYP726A35 chimera for expression in yeast, the length of the plastidial transit sequence was estimated using ChloroP prediction, at about 132 residues. The ER localizing tag of an ER localized C5ox CYP, ElCYP726A27, was annotated by ChloroP and the front 36 residues were used to replace the ChloroP predicted native plastidial transit sequence of JcCYP726A35 (Emanuelsson et al., 1999). The resulting chimeric protein was ordered from IDT.

2.3. Synthetic genes and oligonucleotides

Oligonucleotides and synthetic genes were commercially synthesized (Integrated DNA Technologies, Inc.). All codon optimized sequences were designed based on the IDT online tool. Sequences of synthetic genes can be found in Supplementary Fig. 10.

2.4. Culture and fermentation conditions

Selective agar plates used for transformations were purchased from Teknova (www.teknova.com, cat. C3080). Liquid selective medium used to grow transformants contained 0.2% (w/v) complete supplement mixture (CSM) lacking uracil (www.sunrisescience.com, cat. 1004-100), 0.67% yeast nitrogen base (www.difco.com, cat. 291920), and 2% dextrose. Nonselective medium contained 1% yeast extract, 2% peptone (Difco cat. 288620 and 211677, respectively), and either 2% dextrose (YPD) or 2% galactose and 0.2% dextrose (YPG). Nonselective agar YPD plates were purchased from Teknova (cat. Y100). Cultures were grown in plastic 96-deep well plates (www.vwr.com, cat. 29445-166) and glass test tubes for strain maintenance, while 2 ml of media in 24-deep well plastic plates (CWR cat. 89080-534) were used for all production runs. Production cultures were spiked with 50 mg/L trans-caryophyllene (sigma cat. C9653) as an internal standard. Plastic plates were covered with aeraseal film (www.excelscientific.com, cat. BS-25) and shaken at 800 rpm in a Multitron shaker (www.infors-ht.com, model AJ185). Production runs were cultured for 48 h in 2 ml of YPG before terpenoid extraction for analysis. Glass tubes were shaken at

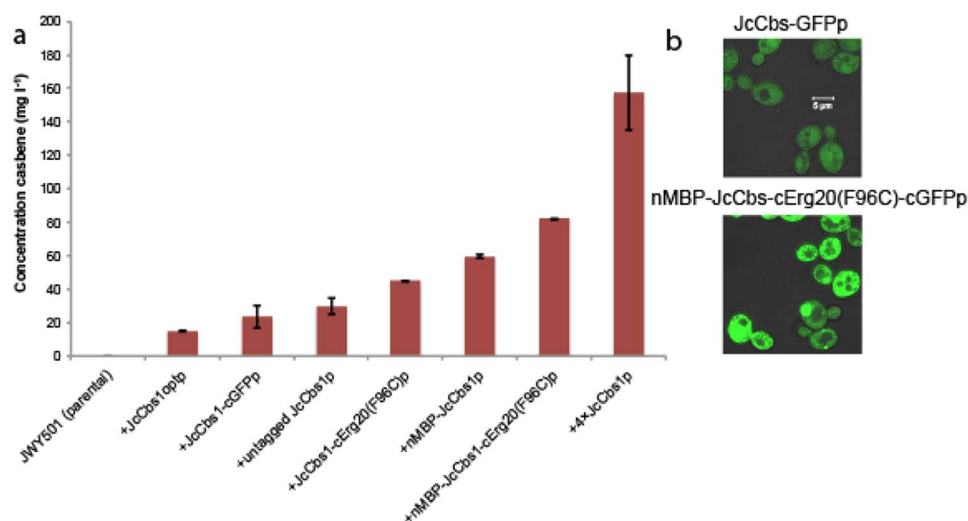


Fig. 2. Engineering casbene production in yeast. (a) Different protein tags attached to *J. curcas* casbene synthase (JcCbs1p) improved casbene titer. All *JcCBS1* variants were integrated into the GGPP-producing parent strain, JWY501. Strain JWY509, containing four copies of *JcCBS1*, was used as the parent for all P450 testing in subsequent studies. Data represent the averages of three biological replicates; error bars show one standard deviation from the mean. The lowercase letter in front of the tag name indicates the terminus of CBS to which the tag was attached, i.e. N- or C-terminus. (b) GFP-tagging experiments with JcCbs1p reveal increased expression and protein stability with solubility tags. Confocal microscopy studies show low expression from a single integrated copy of GFP fused JcCbs1p in yeast (top). A single integrated copy of three tag *JcCBS1* (producing nMBP-JcCbs1-cErg20[F96C]-cGFPp) results in increased expression levels (bottom). Flow cytometry experiments indicate that strains expressing a single copy of three tag *JcCBS1* exhibit nearly three times the fluorescence intensity than strains

expressing one copy of JcCbs1-cGFPp (Supplemental Fig. 8).

200 rpm. All strains were grown at 30 °C.

2.5. Confocal microscopy

To visualize GFP expression of tagged CBS variants in yeast strains, strains were grown in 5 ml YPD overnight, then back-diluted 1:100 into the same medium and grown 3–6 h at 200 rpm and 30 °C. Then, 1 ml of culture volume was centrifuged at 10,000 rpm on a table-top centrifuge, washed with 1x water, and 1 μl of the cell pellet was imaged using a Zeiss LSM 710 confocal system mounted on a Zeiss inverted microscope (www.zeiss.com) with a 63 Å~ objective and processed using Zeiss Zen software.

2.6. Metabolite quantification using GCMS and HPLC-UV

Yeast cultures grown in 2 ml of YPgal in 24-deep well plastic plates for 48 h were extracted 1:1 with EtOAc spiked with 50 mg/L trans-caryophyllene by shaking for 30 min, then spun at 21,952 x g for 1 min. For GC-MS analysis, the resulting organic phase was removed and transferred to GC vials. An aliquot of the sample (1 μL) was injected into a cyclosil B column (J&W Scientific) operating at a He flow rate of 1 ml/min on GC-MS (GC model 6890, MS model 5973 Inert, Agilent). An initial temperature of 120 °C was held for 3 min, followed by ramping to 250 °C at a rate of 20 °C/min to 250 °C, and then held at 250 °C for another 3 min. The total flow was set to 8.3 ml/min and helium flow was set to 1 ml/min. For HPLC analysis, the resulting organic phase was removed and dried down at 54 °C in vacuum, and the extract was redissolved in 500 μL of MeOH. 25 μL of the extract was analyzed on an Agilent HPLC 1200 series using a Zorbax Eclipse XDB-C18 column (Agilent, 5-micron, 4.6 mm × 250 mm), kept at 40 °C. Mobile phases A and B were water and methanol respectively. A flow of 1 ml/min was used. The gradient profile was as follows: 5 min constant at 10% B, a linear gradient from 10% B to 100% B in 10 min, held for 13 min, a second linear gradient from 100% B to 10% B for 1 min, and final step of 10% B maintained for 11 min. The following wavelengths were monitored: 204 nm, 254 nm, 270 nm, and 280 nm, and 270 nm was used for quantification. All production measurements were performed in biological triplicates or quadruplicates. A casbene standard containing known concentrations of the internal standard and casbene extracted from a casbene producing strain was used to determine titer. Farnesol (sigma cat. F203) was used as a standard for singly hydroxylated casbenes, while authentic standards of jolkinol C, 6,9-dihydroxy-5-ketocasbene, and 6-hydroxy-5-ketocasbene were isolated and weighed and verified by H¹ NMR from JWY521 culture to quantify these products of our strains.

3. Results and discussion

3.1. Engineering casbene production in yeast

Past studies have reported casbene production in *S. cerevisiae* by expressing the casbene synthase gene (*CBS*) from plasmids^{22,23}. To date, titers remain under 30 mg/L, hampering development of advanced lathyrane diterpenoid production strains. Previous studies expressing plant-derived diterpene synthases in yeast suggest protein insolubility as a limiting factor in heterologous expression and demonstrated improved activity by tagging with soluble proteins (Reider Apel et al., 2017; Ignea et al., 2015). To develop a strain for high-level production of casbene, we optimized soluble expression of Cbsp using protein tagging strategies. We integrated a truncated version of the gene encoding *Jatropha curcas* Cbsp (*JcCBS1*) alone or with various protein tags into a GGPP-producing strain developed by our group, GTy116 (Reider Apel et al., 2017; Nakano et al., 2012). These tags included a maltose binding protein (MBP, codon-optimized for yeast expression) attached to the N-terminus of JcCbs1p, which led to 15-fold improvement in casbene titers over the untagged JcCbs1p variant (Fig. 2a). Two other constructs, green fluorescent protein (GFP) attached to the C-terminus of JcCbs1p, and a yeast codon-optimized *JcCBS1*, both showed similar casbene titers as the untagged, non-codon optimized JcCbs1p. Ignea and colleagues reported an over 200-fold increase in diterpene production when they expressed a mutated GGPP-producing *S. cerevisiae* *ERG20* variant, *ERG20(F96C)* in a diterpene strain. Fusion of the protein encoded by this gene to the diterpene synthase in their system appeared to improve the titer further, likely due to increased solubility of the terpene synthase (Ignea et al., 2015). We screened the fusion protein JcCbs1-Erg20(F96C)p and saw modest titer improvements. However, a two-tag variant of JcCbs1p with an MBP tag on the N-terminus and an Erg20(F96C)p fusion on the C-terminus outperformed all other JcCbs1p variants, resulting in ~80 mg/L casbene. To examine protein solubility improvement from protein tagging strategies, we developed a 3-tag construct, MBP-JcCbs1-Erg20(F96C)-GFPp, for imaging. This strain showed significantly elevated and disbursed GFP expression within the cell relative to the JcCbs1-GFPp construct, indicating that the MBP tag and Erg20(F96C)p fusion indeed aided expression, possibly due to increased protein stability (Fig. 2b). A strain with three additional copies of *CBS* (hereafter referred to as JWY509) led to a final titer of ~160 mg/L casbene, by far the highest titer of casbene in yeast reported to date.

3.2. Engineering CYP expression in yeast

Besides the synthesis of the diterpene casbene, lathyrane biosynthesis involves CYP-catalyzed oxidation at three positions of the casbene hydrocarbon skeleton, as well as the formation of a C-C bond between carbons 6 and 10 (see numbering scheme in Fig. 1b). We examined CYPs known and hypothesized to act on casbene in our high-titer casbene-producing yeast strain JWY509. CYPs from *J. curcas* and *E. lathyris* reported to act on C-9 of casbene (hereafter referred to as C9OX CYPs) and ones that act on C-5 and C-6 (hereafter referred to as C5OX CYPs) were co-integrated with a CPR—required for channelling electrons from NADPH to the CYP heme domain—found in the transcriptome of *J. curcas*, hereafter referred to as *JcCPR1* (Luo et al., 2016; King et al., 2016). We used *JcCpr1p* for both the *E. lathyris* and *J. curcas* CYPs because it has been shown that plant P450-CPR interacting domains are highly conserved across plants species, and previous studies have had success using non-cognate CPRs within *Euphorbiaceae* for functional testing of casbene C9OX and C5OX CYPs (Luo et al., 2016; Jensen and Möller, 2010).

JWY509 cultures expressing C9OX CYPs and *JcCpr1p* produced 9-hydroxycasbene, 9-ketocasbene, or a mixture of both, as identified by GC-EIMS fragmentation patterns (Fig. 3, Supplementary Fig. 2). Additionally, we decided to test the CYP gene adjacent to the *C9OX2* in the published *J. curcas* jolkinol C biosynthetic gene cluster (Supplementary Fig. 1) (King et al., 2016). This enzyme, *JcC9OX1p*, whose activity was not previously reported, showed low-level activity on casbene at the C-9 position when expressed in our casbene-producing yeast strain. Of the C9OX CYPs tested, the most productive enzyme was the codon-optimized *E. lathyris* ELC9OX1p, which consumed 90% of the casbene relative to the parental strain, while producing more than 44 mg/L of C-9 oxidized casbanes. The most productive enzyme from *J. curcas* was *JcC9OX2p* (in JWY511), which consumed 70% of the casbene relative to the parental strain, while producing 35 mg/L C-9 oxidized casbene. Interestingly, ELC9OX1p produced primarily 9-hydroxycasbene, while the other C9OX candidates produced a relatively equal mix of the 9-ketocasbene and 9-hydroxycasbene intermediates (Supplementary Fig. 3). Due to ELC9OX1p showing both the highest total C-9 oxidation activity, as well as product specificity for 9-hydroxycasbene—our desired intermediate—we chose this strain for further pathway engineering.

One of the C5OX CYPs, *JcC5OX1p*, has been shown to localize to the plastidial membrane rather than the endoplasmic reticulum when heterologously expressed in *N. benthamiana* (King et al., 2016). To test the expression of this CYP in yeast, we designed a chimeric version of the enzyme by replacing the predicted N-terminus plastidial transit sequence with the beginning of the ER-targeting ELC5OX1p sequence. The

resulting chimeric protein was a similar length to the non-plastid localizing C5OX CYPs (Emanuelsson et al., 1999) (Supplementary Fig. 10).

Upon expressing C5OX CYPs in JWY509, we noticed the production of 5-ketocasbene as well as 6-hydroxy-5-ketocasbene from only *JcC5OX2p*, which is consistent with a previous report using the *N. benthamiana* expression system (King et al., 2016) (Fig. 3b). Both other C5OX CYPs produced only 5-ketocasbene at lower titers.

3.3. Combining C9OX and C5OX CYPs to produce jolkinol C

After we found the most productive C9OX and C5OX CYPs, we decided to test our C5OX CYPs in the best C9OX CYP strain, JWY512, for production of the desired product jolkinol C. It was unclear what the products of coexpressing C5OX CYPs in strain JWY512 would be, given that previous studies disagree on this matter (Luo et al., 2016; King et al., 2016). Despite detecting jolkinol C in *N. benthamiana* when expressing *E. lathyris* C9OX CYP and C5OX CYP, coexpressing these enzymes in yeast did not result in the production of jolkinol C, but rather the formation of primarily 5-hydroxy-9-ketocasbene, a purported dead-end product (Luo et al., 2016). This result may be attributed to differences in pH or some intracellular environmental condition responsible for the ring closure in plant cells that is different in yeast cells. We therefore tested C9OX CYP and C5OX CYP combinations in yeast and analyzed product profiles by GC-MS, HPLC, and NMR (Supplementary Fig. 4, 5, and 6). HPLC-UV analysis was possible since casbanes and lathyrans with α,β -unsaturated carbonyls absorb in the 270–290 nm range (Seip and Hecker, 1983). Indeed, when these samples were run on HPLC, we saw the appearance of three major peaks, which NMR analysis showed were 6-hydroxy-5-ketocasbene, 6,9-dihydroxy-5-ketocasbene (proposed to be the final intermediate before jolkinol C in the *J. curcas* pathway) and (in one strain) jolkinol C (Supplementary Fig. 5). The only C5OX CYP that produced detectable jolkinol C when expressed in JWY512 was *JcC5OX2p*, producing ~360 mg/L jolkinol C. (Fig. 4). The chimeric *JcC5OX1p* did not produce any detectable jolkinol C.

We co-integrated the best C9OX CYP and C5OX CYP from *J. curcas*, surmising that P450s from the same species may cooperate to produce higher levels of jolkinol C. This strain, JWY519, produced a slightly higher level of jolkinol C (400 mg/L) than the cross-species pair (JWY518). Thus, we used this strain for further strain development (Fig. 4).

3.4. ADH's role in jolkinol C production and strain engineering to improve jolkinol C titer

Previous studies on lathyrane diterpenoid biosynthesis have

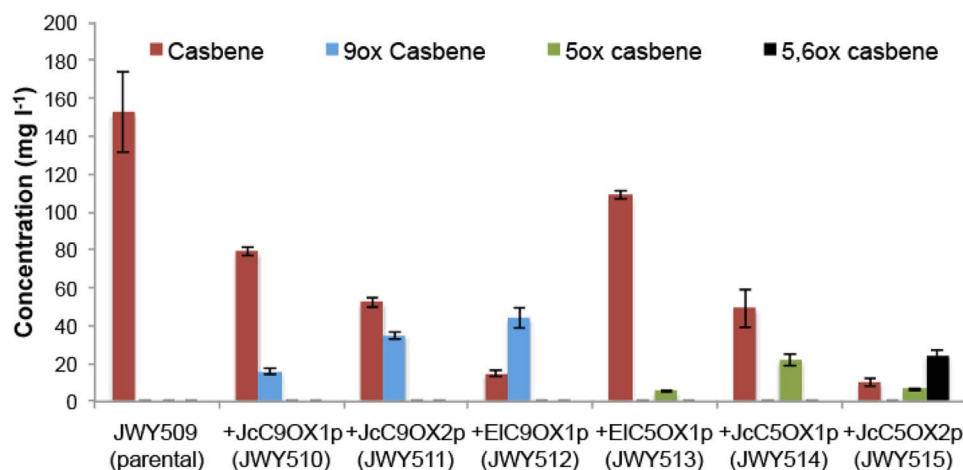


Fig. 3. Titers of casbene, singly- and doubly-oxidized casbanes (sum of hydroxy and keto forms), detected in the presence of different C9OX and C5OX CYP variants. All CYP variant constructs were individually co-integrated with the *J. curcas* CPR (*JcCPR1*) into the high titer casbene strain JWY509. The formation of 9-ketocasbene has been shown to be a dead-end product and is likely due to over-activity of C9OX on an accumulating 9-hydroxycasbene, resulting in double oxidation at the C-9 position. We presume that 9-hydroxycasbene will be consumed in the presence of a C5OX CYP (Luo et al., 2016), so we estimated CYP activity by the combined accumulation of C-9 oxidized casbanes. Cultures were extracted after 48 h and analyzed for oxidized casbane production by GC-MS. ELC9OX1p outperforms all C9OX CYPs in C-9-oxidized casbene production, while *JcC5OX2p* outperforms all the other C5OX CYPs in production of C-5/C-6 oxidized casbene. Data represent the averages of three replicate cultures; error bars show s.d.

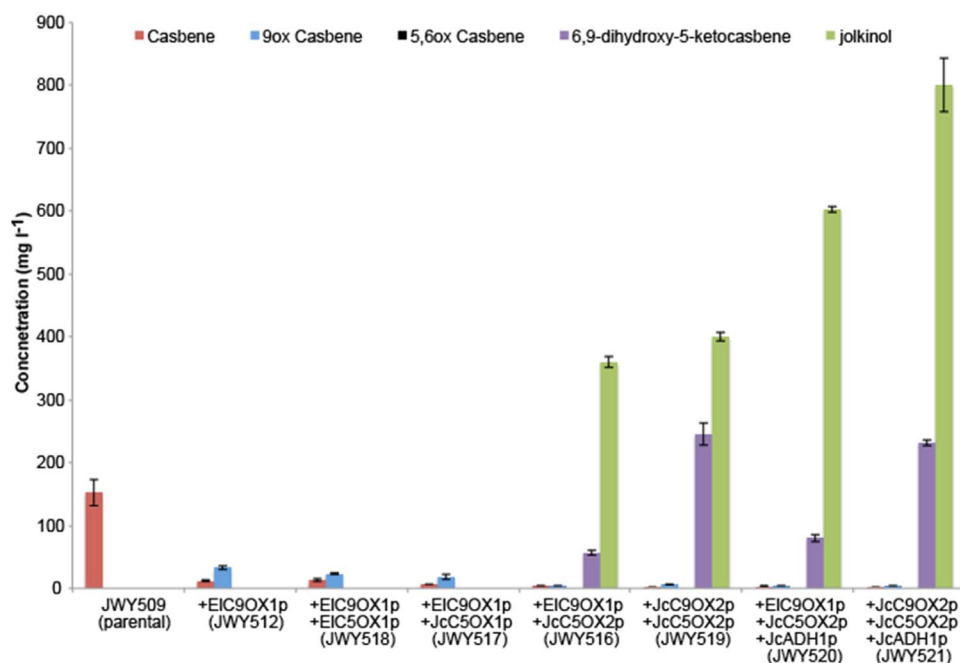


Fig. 4. Production of 6,9-hydroxy-5-ketocasbene and jolkinol C with various combinations of C9OX CYP, C5OX CYP, and ADH variants. C5OX CYPs were screened for jolkinol C production when expressed with the most productive C9OX CYP, EIC9OX1p. Only JcC5OX2p formed any detectable level of jolkinol C. Additionally, we integrated this CYP into the best *J. curcas* C9OX CYP parental strain containing JcC9OX2p. It is important to note that EIC5OX1p produced low titers of C-5 oxidized casbanes in JWY509 and produced low levels of 9-keto-5-hydroxycasbene, a purported dead end product, while producing no triply oxidized casbanes nor jolkinol C. All strains were cultured in 2 ml of YPG medium in milliliter plates, grown for 48 h, and the culture medium analyzed for casbene (red bars) and C-9 oxidized casbene (blue bars) by GC-MS, while all other compounds were measured by HPLC-UV. Bars represent mean values \pm 1 sd. of three replicate cultures. All compounds were quantified using authentic standards purified from high-producing strains.

suggested the involvement of *Euphorbiaceae* ADHs in the formation of jolkinol C. One study found an *E. lathyris* ADH (ElAdh1p) was required for jolkinol C production *in vitro* and *in planta* (Luo et al., 2016) (Luo et al., 2016). Another group working on the *J. curcas* pathway reported jolkinol C production in the absence of an ADH, despite a homolog of ElAdh1p being present in a *J. curcas* gene cluster (NW_012124159) containing jolkinol C biosynthetic genes including *JcCBS1*, *C9OX*, and *C5OX* (King et al., 2016). We thus sought to determine the role of ADH in the formation of jolkinol C in yeast.

We proceeded to test native and codon-optimized forms of *ElADH1* and *JcADH1* in our top jolkinol C producers JWY518 and JWY519. We found that all integrated ADHs drastically improved jolkinol C titer by about 2-fold (Fig. 3), and increased the levels of the non-ring closed accumulated intermediate, 6,9-dihydroxy-5-ketocasbene. The jolkinol production levels from strains containing the two ADHs from the two species did not differ statistically and neither codon optimization nor protein-tagging of the ADHs further improved titer (Supplementary Fig. 7). While testing different cultivation conditions for jolkinol C production, we noticed a consistent increase in titers of jolkinol C and oxidized casbane intermediates when higher surface area:volume ratios or higher agitation rates were used, likely due to increased oxygen supply improving CYP activity (Supplementary Fig. 7). This indicates a need for additional strain and process engineering for industrial applications. Our final top producing strain, JWY521, produced 801 mg/L \pm 42 mg of jolkinol C. This high titer illustrates the promise of using engineered yeast for further gene discovery of related pathways, circumventing the problem of low yield often associated with gene functional testing using other techniques.

4. Conclusions

Diterpenoid drugs have a long history of success in medicine. Although discovery of biosynthetic pathways can be arduous, we believe that applying the techniques used in this work in yeast can provide a stable biosynthetic platform for accelerated gene discovery for valuable FDA-approved compounds such as ingenane-3-angelate and taxol. These natural products are often difficult to source in quantities necessary for drug clinical trials due to the large number of chiral centers, which make efficient chemical synthesis difficult, and low yields from plant cell culture or farmed plants. We believe that protein tagging

strategies, optimizing copy number, and screening libraries of enzymes from different species that perform the same reaction can allow one to find the optimal combinations of terpenoid biosynthetic genes for industrial drug production in yeast strains, particularly for oxygenated compounds.

Our data conclusively show that EIC9OX1p and JcC5OX2p co-expressed alongside an ADH allow for the biosynthesis of the important lathyrene precursor jolkinol C. This pathway illustrates the potential of combinatorial CYP screening and the use of yeast to characterize CYP expression in terpenoid biosynthetic pathways. The final engineered jolkinol C strain (JWY521) produced 800 mg/L jolkinol C. These titers highlight the advantage of yeast as a host over the previously used transient expression in *N. benthamiana* for gene discovery. The extraction of jolkinol C from this yeast chassis greatly simplifies gene discovery of the pathway, while using *N. benthamiana* as an expression host requires harvesting and extracting many plants and performing many downstream isolation steps to produce enough jolkinol C for gene discovery. Additionally, the methods used in the paper are advantageous over previous terpenoid gene discovery methods in yeast, as previous groups have relied on high-copy number plasmids, which suffer from plasmid instability, high levels of expression variability, and the limited number of genes that can be expressed from such a system (Kirby et al., 2010; Luo et al., 2016; Ro et al., 2006).

Because previous studies have suggested yeast codon-optimization of CYPs improved titer of target compounds, we used all codon-optimized CYPs (Paddon et al., 2013; Luo et al., 2016). However, we decided to test whether this trend was consistent in the downstream pathway enzymes, the ADHs. Interestingly, the codon-optimized ADH strains did not outperform their non codon-optimized counterparts. However, we believe that codon optimization can be used as a general strategy for improving enzyme expression in diterpenoid pathways.

The necessity of an ADH for the formation of jolkinol C has been debated. However, our work shows that although the ADHs tested greatly improve jolkinol C production, they are not necessary for production of jolkinol C. These findings resolve the differences seen in King and Luo's experiments. King and colleagues produced jolkinol C by transient expression of CBS, C9OX CYP and C5OX CYP in *N. benthamiana* and did not require the use of an ADH, while Luo and colleagues only saw the formation of jolkinol C in the presence of ElAdh1p *in vitro* and *in planta* (Luo et al., 2016; King et al., 2016).

The lack of jolkinol C production in the *E. lathyris* system in the absence of an ADH is likely due to the low activity of EIC5OX1p on the C-6 position of the casbene skeleton, even when coexpressed with a C9OX CYP. To this effect, our strain JWY518 produced a doubly oxidized casbene, shown to be 9-keto-5-hydroxycasbene by Luo and colleagues, which is a dead-end product (Supplementary Fig. 3).

Based on *in vitro* data reported by Luo and colleagues, we believe that the ADH converts 6,9-dihydroxy-5-ketocasbene to 6-hydroxy-5,9-diketocasbene, which is poised for spontaneous cyclization into jolkinol C. Perhaps, the *J. curcas* CYPs have some ability to effect a second oxidation on the C-9 position of the intermediate 6,9-dihydroxy-5-ketocasbene and thus produce detectable levels of jolkinol C in the absence of an ADH. The dramatic jolkinol C titer improvements in the ADH strains supports the direct involvement of an ADH in jolkinol C biosynthesis.

The ADH integrations caused a massive increase in jolkinol C titers, while roughly maintaining titers of the precursor 6,9-dihydroxy-5-ketocasbene. We cannot explain the massive total diterpenoid titer increase in the jolkinol C-producing strains relative to the casbene- and singly/doubly oxidized casbene-producing strains. It is possible that the triply oxidized casbanes and lathyranes are less cytotoxic than casbene and singly or doubly hydroxylated casbene.

Our work significantly advances the field of diterpenoid biosynthesis in yeast and specifically for jolkinol C, for which we engineered the biosynthetic steps required for its heterologous production. This jolkinol C chassis strain will significantly simplify discovery of additional genes in the biosynthetic pathways of ingenol-3-angelate and tiglianes such as prostratin. This work represents the highest levels of oxidized diterpenoids produced to date in any microorganism.

Acknowledgements

The DOE Joint BioEnergy Institute is supported by the US Department of Energy, Office of Science, Office of Biological and Environmental Research, through contract DE-AC02-05CH11231.

Competing financial interests

J.D.K. has financial interests in Amyris, Lygos, and Dematrix.

Author contributions

J.W., J.D.K., and J.K. conceived this project. J.W., L.d'E., T.d.R. and H.S. designed all of the experiments. J.W., L.d'E., L.R.S., C.v.d.H., and I.D. constructed all strains. J.W., L.d'E., and T.d.R. performed all analytical measurements. T.d.R. isolated and identified compounds and performed analytical chemistry techniques for all compounds. J.W., L.d'E., and T.d.R. analyzed the data. J.W. wrote the paper.

Appendix A. Supporting information

Supplementary data associated with this article can be found in the online version at <http://dx.doi.org/10.1016/j.ymben.2017.12.007>.

References

Amiri, P., Shahpiri, A., Asadollahi, M.A., Momenbeik, F., Partow, S., 2016. Metabolic engineering of *Saccharomyces cerevisiae* for linalool production. *Biotechnol. Lett.* 38, 503–508.

Andersen-Ranberg, J., et al., 2016. Expanding the landscape of diterpene structural diversity through stereochemically controlled combinatorial biosynthesis. *Angew. Chem. Int. Ed. Engl.* 55, 2142–2146.

Emanuelsson, O., Nielsen, H., Heijne, G.V., Chlora, P., 1999. A neural network-based method for predicting chloroplast transit peptides and their cleavage sites | *Protein Science* | Cambridge Core. *Protein Sci.* at <https://www.cambridge.org/core/journals/protein-science/article/chlorop-a-neural-network-based-method-for-predicting-chloroplast-transit-peptides-and-their-cleavage-sites/A4CFAC2436726045600012D2F8C22DF0>.

Gietz, R.D., Woods, R.A., 2002. Screening for protein-protein interactions in the yeast two-hybrid system. *Methods Mol. Biol.* 185, 471–486.

Halaweish, F.T., Kronberg, S., Hubert, M.B., Rice, J.A., 2002. Toxic and aversive diterpenes of *Euphorbia esula*. *J. Chem. Ecol.* 28, 1599–1611.

Ignea, C., et al., 2011. Improving yeast strains using recyclable integration cassettes, for the production of plant terpenoids. *Microb. Cell Fact.* 10, 4.

Ignea, C., et al., 2015. Efficient diterpene production in yeast by engineering Erg20p into a geranylgeranyl diphosphate synthase. *Metab. Eng.* 27, 65–75.

Ignea, C., Pontini, M., Maffei, M.E., Makris, A.M., Kampranis, S.C., 2014. Engineering monoterpene production in yeast using a synthetic dominant negative geranyl diphosphate synthase. *ACS Synth. Biol.* 3, 298–306.

Jensen, K., Möller, B.L., 2010. Plant NADPH-cytochrome P450 oxidoreductases. *Phytochemistry* 71, 132–141.

Jiao, W., Dong, W., Li, Z., Deng, M., Lu, R., 2009. Lathyrene diterpenes from *Euphorbia lathyris* as modulators of multidrug resistance and their crystal structures. *Bioorg. Med. Chem.* 17, 4786–4792.

Johnson, H.E., Banack, S.A., Cox, P.A., 2008. Variability in content of the anti-AIDS drug candidate prostratin in Samoan populations of *Homalanthus nutans*. *J. Nat. Prod.* 71, 2041–2044.

Jongedijk, E., et al., 2015. Capturing of the monoterpene olefin limonene produced in *Saccharomyces cerevisiae*. *Yeast* 32, 159–171.

King, A.J., et al., 2016. A Cytochrome P450-Mediated Intramolecular Carbon-Carbon Ring Closure in the Biosynthesis of Multidrug-Resistance-Reversing Lathyrene Diterpenoids. *ChemBiochem* 17, 1593–1597.

Kirby, J., et al., 2010. Cloning of casbene and neocembre synthases from *Euphorbiaceae* plants and expression in *Saccharomyces cerevisiae*. *Phytochemistry* 71, 1466–1473.

Luo, D., et al., 2016. Oxidation and cyclization of casbene in the biosynthesis of *Euphorbia* factors from mature seeds of *Euphorbia lathyris* L. *Proc. Natl. Acad. Sci. USA* 113, 5082–5089.

Nakano, Y., et al., 2012. Characterization of the casbene synthase homolog from *Jatropha* (*Jatropha curcas* L.). *Plant Biotechnol.* 29, 185–189.

Paddon, C.J., et al., 2013. High-level semi-synthetic production of the potent antimalarial artemisinin. *Nature* 496, 528–532.

Payne, C.K., et al., 2005. Intravesical resiniferatoxin for the treatment of interstitial cystitis: a randomized, double-blind, placebo controlled trial. *J. Urol.* 173, 1590–1594.

Reider Apel, A., et al., 2017. A Cas9-based toolkit to program gene expression in *Saccharomyces cerevisiae*. *Nucleic Acids Res* 45, 496–508.

Renault, H., Bassard, J.-E., Hamberger, B., Werck-Reichhart, D., 2014. Cytochrome P450-mediated metabolic engineering: current progress and future challenges. *Curr. Opin. Plant Biol.* 19, 27–34.

Ro, D.-K., et al., 2006. Production of the antimalarial drug precursor artemisinic acid in engineered yeast. *Nature* 440, 940–943.

Seip, E.H., Hecker, E., 1983. Lathyrene type diterpenoid esters from *Euphorbia characias*. *Phytochemistry* 22, 1791–1795.

Selling Forest Environmental Services, 2012. Market-Based Mechanisms for Conservation and Development. Taylor & Francis.

Shimokawa, K., Takamura, H., Uemura, D., 2007. Concise synthesis of a highly functionalized cyclopentane segment: toward the total synthesis of kansuiniine A. *Tetrahedron Lett.* 48, 5623–5625.

Siller, G., Gebauer, K., Welburn, P., Katsamas, J., Ogbourne, S.M., 2009. PEP005 (ingenol mebutate) gel, a novel agent for the treatment of actinic keratosis: results of a randomized, double-blind, vehicle-controlled, multicentre, phase IIa study. *Australas. J. Dermatol.* 50, 16–22.

Srivalli, K.M.R., Lakshmi, P.K., 2012. Overview of P-glycoprotein inhibitors: a rational outlook. *Braz. J. Pharm. Sci.* 48, 353–367.

Tamino, K., et al., 2003. Total synthesis of ingenol. *J. Am. Chem. Soc.* 125, 1498–1500.

Trippa, F.A., et al., 2015. Iterative carotenogenic screens identify combinations of yeast gene deletions that enhance sclareol production. *Microb. Cell Fact.* 14, 60.

Vasas, A., Hohmann, J., 2014. *Euphorbia* diterpenes: isolation, structure, biological activity, and synthesis (2008–2012). *Chem. Rev.* 114, 8579–8612.

Wang, H.-B., Wang, X.-Y., Liu, L.-P., Qin, G.-W., Kang, T.-G., 2015. Tigliane diterpenoids from the *Euphorbiaceae* and *Thymelaeaceae* families. *Chem. Rev.* 115, 2975–3011.

Wender, P.A., McDonald, F.E., 1990. Studies on tumor promoters. 9. A second-generation synthesis of phorbol. *J. Am. Chem. Soc.* 112, 4956–4958.

Wender, P.A., Kee, J.-M., Warrington, J.M., 2008. Practical synthesis of prostratin, DPP, and their analogs, adjuvant leads against latent HIV. *Science* 320, 649–652.

Westfall, P.J., et al., 2012. Production of amorphadiene in yeast, and its conversion to dihydroartemisinic acid, precursor to the antimalarial agent artemisinin. *Proc. Natl. Acad. Sci. USA* 109, E111–E118.